Journal of Materials Chemistry B

PAPER

View Article Online
View Journal | View Issue

Cite this: J. Mater. Chem. B, 2014, 2, 5220

Low temperature preparation of a graphene–cobalt microsphere hybrid by borohydride-initiated reduction for enriching proteins and peptides†

Huimin Ge, Huimin Bao, Luyan Zhang and Gang Chen*

Received 23rd February 2014
Accepted 16th June 2014

DOI: 10.1039/c4tb00302k

www.rsc.org/MaterialsB

A graphene–cobalt microsphere hybrid was prepared by the chemical reduction of a mixture containing graphene oxide and cobalt chloride. It was found that a little amount of potassium borohydride or sodium borohydride could initiate the hydrazine-reduction of the mixture at a low temperature of 80 °C. The structure of the material was investigated by scanning electron microscopy, transmission electron microscopy, energy dispersive spectroscopy, vibrating sample magnetometery, Fourier transform infrared spectroscopy, Raman spectroscopy, and Brunauer–Emmett–Teller (BET) techniques. The average size of the cobalt microspheres on graphene sheets was measured to be ~590 nm. Magnetic investigations indicated that the graphene–cobalt microsphere hybrid exhibited ferromagnetic behavior at room temperature. In addition, the magnetic hybrid was successfully employed in the enrichment and identification of low-abundance proteins and peptides in combination with mass spectrometry.

1. Introduction

As an important allotrope of carbon, graphene has a two-dimensional nanostructure of sp^2-bonded carbon atoms that are arranged in a honeycomb pattern.[1,2] Since it was successfully isolated and characterized by Novoselov and Geim in 2004, graphene has received ever-increasing attention and become a rapidly rising star in the fields of materials sciences and condensed-matter physics owing to its unique two-dimensional structure and excellent physical and chemical properties.[3–9]

Nowadays, graphene is mainly prepared by chemical reduction of graphene oxide (GO), chemical vapor deposition from carbon precursors, and exfoliation of graphite by a variety of approaches.[10] Among them, the first approach is commonly used to produce graphene at low cost. Because GO sheets bear a great deal of oxygen-containing groups, they can be well dispersed in aqueous solution for the preparation of graphene-based hybrids.[11] When GO sheets are reduced to hydrophobic graphene sheets in aqueous solution, they tend to aggregate to form graphitic structures under the drive of the interlayer π–π interaction, van der Waals force, and hydrophobic interaction. To solve the problem, a variety of inorganic particles are decorated on graphene sheets to enlarge the interplanar spacing between them. A series of graphene-based hybrids have been prepared by decorating them with the particles of Cu,[8] Au,[12] Ag,[13] Pt,[14] ZnS,[15] MnO_2,[16] NiO,[17] *etc.* In the past few decades, various approaches have been developed for the preparation of cobalt particles owing to their unusual magnetic properties and industrial importance.[18,19] Because exfoliated graphene sheets have a large specific surface area (2600 m^2 g^{-1} (ref. 20)) and unique properties, it is interesting to deposit cobalt particles on them to prepare magnetic hybrids. To date, graphene–cobalt hybrids are mainly prepared by high-temperature hydrogen reduction,[21,22] hydrothermal treatment,[23,24] solvothermal method,[25,26] sol–gel autocombustion,[27] flame spray pyrolysis,[28] chemical vapor deposition,[29] mechanical ball milling,[30] and electrodeposition.[31] Besides the last two methods, other approaches need to be performed at high temperatures in the range of 180 to 800 °C. It is of high importance to develop efficient approaches for the rapid preparation of the magnetic graphene–cobalt hybrid in aqueous solution at low temperatures.

Proteomics is the large-scale study of proteins, particularly their structures and functions. As one of the fastest developing areas in biological research, proteomics has drawn more and more attention.[32,33] One of its most important tasks is to develop efficient and rapid approaches to identify various proteins. Peptide mapping is a commonly used strategy for protein identification. Proteins are usually digested into peptides that are subsequently identified by matrix-assisted laser desorption/ionization time-of-flight mass spectrometry (MALDI-TOF MS) along with database searching.[34] Although MALDI-TOF MS is highly sensitive, it is usually insufficient for the detection of low-abundance peptides or proteins isolated from biological samples. Prior to MS analysis, a prior enrichment of the samples is usually inevitable. Because magnetic nanomaterials

School of Pharmacy, Department of Chemistry, Fudan University, 826 Zhangheng Road, Shanghai 201203, China. E-mail: gangchen@fudan.edu.cn; Fax: +86-21-51980168; Tel: +86-21-51980061

† Electronic supplementary information (ESI) available. See DOI: 10.1039/c4tb00302k

can be easily manipulated with the aid of external magnetic fields, they indicate great promise for the enrichment of proteins and peptides in proteomics research.[34–36] A variety of novel magnetic nanomaterials were synthesized by assembling various materials on magnetic iron oxide microspheres followed by surface modification.[34–36] Recently, graphene nanosheets were covalently attached on silica particles[37] and magnetic iron oxide spheres[38] for the enrichment of proteins and peptides. However, to the best of our knowledge, no adsorbent composed of metallic cobalt and graphene sheets has been reported for enriching peptides and proteins.

In this work, a graphene–cobalt microsphere (CoMS) hybrid was prepared by the chemical reduction of GO sheets and cobalt(II) chloride in a hydrazine-containing solution at a lower temperature of 80 °C. It was demonstrated that a little amount of potassium borohydride or sodium borohydride could initiate the reduction reaction and the reduction time was reduced to as short as 60 min. In addition, the prepared hybrid was employed in the enrichment and identification of low-abundance proteins and peptides in combination with MALDI-TOF MS. It exhibits excellent magnetic responsibility and enrichment capability. In the prepared hybrid, hydrophobic graphene nanosheets with high specific surface area can capture the proteins and peptides in solution while its cobalt component facilitates rapid magnetic separation. The MALDI-TOF-MS signals of low-abundance proteins and peptides are substantially enhanced after enriching with the unique magnetic hybrid. The preparation details, characterization, advantages, and application of the graphene–CoMS hybrid are reported in the following sections.

2. Experimental

2.1. Reagents and solutions

Cobalt(II) chloride hexahydrate ($CoCl_2 \cdot 6H_2O$), hydrazine hydrate (85% w/w), potassium borohydride, sodium borohydride, graphite powder, potassium permanganate, sodium nitrate, ammonium hydroxide solution (the content of NH_3, 25–28% w/w), hydrogen peroxide solution (30% w/w), and sulfuric acid (98% w/w) were all supplied by SinoPharm (Shanghai, China). Cytochrome c (Cyt-c) from horse heart, lysozyme (LYZ) from chicken egg, bovine hemoglobin (HEM), trypsin from bovine pancreas, trifluoroacetic acid (TFA), acetonitrile (ACN) and α-cyano-4-hydroxycinnamic acid (CHCA) were supplied by Sigma (St. Louis, MO, USA). The stock solutions of Cyt-c, LYZ, and HEM (1 mg mL^{-1}) were prepared in 10 mM NH_4HCO_3 solution (pH 8.1) and were denatured in a 95 °C water bath for 15 min.

2.2. Preparation of oxidized graphite

Oxidized graphite was synthesized from graphite by a modified Hummers method.[12] Briefly, 2 g graphite powder was dispersed in 46 mL of sulfuric acid (98% w/w) under agitation. Subsequently, 1.2 g sodium nitrate and 6 g potassium permanganate were successively added into the mixture in an ice bath. Note that both compounds should be added slowly to prevent the temperature from exceeding 20 °C. After the reaction was allowed to proceed in a 35 °C water bath for 30 min, 92 mL of doubly distilled water was gradually added. The temperature of the mixture was kept at 98 °C for 40 min to increase the oxidation degree of the product. And then, the volume of the resultant suspension was adjusted to 280 mL with doubly distilled water. After 6 mL of hydrogen peroxide solution (30% w/w) was added, the color of the suspension changed from brown to bright-yellow. The prepared oxidized graphite could be easily isolated from the solution by vacuum filtration. The sulfuric acid and salt impurities in the crude product were removed by washing with 5% (w/w) hydrochloric acid and doubly distilled water with the aid of vacuum filtration. The wet product was dewatered by vacuum drying (50 °C).

2.3. Preparation of the graphene–CoMS hybrid

To prepare the graphene–CoMS hybrid, 0.3 g oxidized graphite powder was dispersed in 100 mL doubly distilled water and sonicated in an ultrasonic cleaner (SKQ-2200, frequency 56 kHz, 100 W) for 1 h to exfoliate oxidized graphite particles to GO sheets. After an aqueous solution (5 mL) of $CoCl_2 \cdot 6H_2O$ (1.19 g, 5 mmol) was added, the mixture was sonicated for 10 min. And then, 5 mL of hydrazine hydrate (85% w/w) and 10 mL of ammonium hydroxide solution (the content of NH_3, 25–28% w/w) were successively added into the mixture that was vigorously stirred. The mixture solution was then heated in an 80 °C water bath for 10 min. To initiate the hydrazine-based reduction reaction, 20 mg potassium borohydride (or 15 mg sodium borohydride) was directly dissolved in the mixture with the aid of mechanical agitation. It could be observed that the color of the mixture immediately turned from brown to black while a great deal of colorless gas released from the solution. The reduction reaction was allowed to proceed at 80 °C for 60 min. The obtained graphene–CoMS hybrid could be easily isolated form the solution by vacuum filtration and was purified by washing with copious amounts of doubly distilled water. Finally, it was washed with absolute ethanol and dried in a vacuum. Based on the thermogravimetric analysis (TGA) of the hybrid, the weight ratio of metallic cobalt to graphene within the hybrid was estimated to be approximately 2 : 1.

CoMSs were also prepared by mixing an aqueous solution (20 mL) of $CoCl_2 \cdot 6H_2O$ (1.19 g, 10 mmol) with the solution mixture of 3 mL of hydrazine hydrate (85% w/w) and 10 mL of ammonium hydroxide solution (the content of NH_3, 25–28% w/w). The prepared mixture was heated in an 80 °C water bath for 10 min. And then, 20 mg potassium borohydride was dissolved in the mixture to initiate the reduction reaction. After 30 min, CoMSs could be easily separated from the solution with the aid of an NdFeB magnet (~3000 Gs). Graphene was prepared by the reduction of GO sheets with hydrazine hydrate as a reducing agent.[8]

2.4. Apparatus

The surface morphologies were studied and energy dispersive spectroscopy (EDS) spectra of the prepared materials were recorded by using a scanning electron microscope (PHILIPS XL 30, Eindhoven, The Netherlands). Transmission electron

microscopy (TEM) images were observed using a JEOL model JEM-2011(HR) transmission electron microscope (JEOL Ltd., Japan) at 200 kV. X-ray diffraction (XRD) measurements were carried out using a Rigaku D/max-rB diffractometer (Rigaku, Tokyo, Japan) with CuK-α1 radiation (40 kV, 60 mA). A vibrating-sample magnetometer (Model 155, EG&G Princeton Applied Research, USA) was used at room temperature to study the magnetic properties of the magnetic materials. TGA was performed by using a PerkinElmer Pyris 1 DTA-TGA instrument in air at a heating rate of 10 °C min^{-1}. Raman spectra were acquired on a Labram-1B (Dilor, France) confocal microscopy Raman spectrometer with a 632.8 nm wavelength incident laser light. The Fourier transform infrared (FT-IR) spectra of GO, graphene, CoMS, and graphene–CoMS hybrid were recorded using a FT-IR spectrometer (NEXUS470, NICOLET). Nitrogen adsorption–desorption isotherms were measured with a QuadraSorb SI surface area and pore size analyzer (Quantachrome Instruments, Florida, USA) at 77 K. The specific surface area of the prepared materials was calculated by the Brunauer–Emmett–Teller (BET) method in the relative pressure range of 0.03 to 0.30. The pore size distribution of the materials was calculated by the Barrett–Joyner–Halenda (BJH) approach based on the desorption branches of the isotherms. Prior to the measurements, all samples were degassed at 250 °C under vacuum for 3 h. All MALDI-TOF-MS measurements were performed in positive ion mode using a 5800 proteomics analyzer (Applied Biosystems, Framingham, MA).

2.5. Enrichment of proteins by the graphene–CoMS hybrid

An accurate amount (100 mg) of the prepared graphene–CoMS hybrid was dispersed in 10 mL doubly distilled water with the aid of sonication. The suspension of the magnetic hybrid or pristine CoMSs (10 mg mL^{-1}, 20 μL) was added to 1 mL of mixture solution of Cyt-c and LYZ (1 ng μL^{-1} each) in a polypropylene centrifuge tube. Subsequently, the mixture was shaken for 5 min at ~25 °C. An NdFeB magnet was used to attract the magnetic hybrid to the bottom of the vial. After the clear supernatant was decanted, the protein-captured hybrid was rinsed with water twice and redispersed in 10 μL of 50% aqueous ACN containing 0.1% TFA with the aid of the magnet. The eluent containing enriched proteins was collected for subsequent MS analysis.

2.6. Enrichment of peptides by the graphene–CoMS hybrid

HEM and Cyt-c were digested into peptides following a previously reported procedure.[39] Briefly, the stock solutions of trypsin (1 mg mL^{-1}) were prepared in 50 mM acetic acid aqueous solution. For tryptic digestion, the stock solution of HEM and Cyt-c (200 μL) was mixed with 5 μL trypsin solution and 795 μL of 10 mM NH_4HCO_3 solution (pH 8.1) and incubated at 37 °C for 18 h. The weight ratio of trypsin to protein substrate was 1 : 40. An accurate volume (25 μL) of each digest was further diluted with doubly distilled water to 10 mL to prepare the sample solution (0.5 ng μL^{-1} for each protein) for subsequent enrichment and MALDI-TOF-MS analysis. To demonstrate the enrichment capability of the graphene–CoMS hybrid, 1 mL of each sample solution was mixed with 20 μL of 10 mg mL^{-1} hybrid suspension in a 1.5 mL centrifuge tube that was vibrated for 5 min at ~25 °C. The peptide-captured hybrid was separated and rinsed with water with the aid of a magnet. The adsorbed peptides could be extracted with 10 μL of 50% aqueous ACN containing 0.1% TFA with the aid of the magnet for subsequent MS analysis.

2.7. MALDI-TOF-MS analysis

Prior to MALDI-TOF-MS analysis, each sample (0.5 μL) was spotted on a MALDI plate. After the solvent was evaporated, 0.5 μL of matrix solution (50% aqueous ACN containing 4 mg mL^{-1} CHCA and 0.1% TFA) was dropped on it. The MS instrument was operated at an accelerating voltage of 20 kV. A 1000 Hz pulsed Nd:YAG laser at 355 nm was used. Prior to use, the MS instrument was calibrated with the tryptic digest of myoglobin in an internal calibration mode. Reflector mode was used to detect low-mass peptides while high-mass proteins were measured in a linear mode. GPS Explorer software from Applied Biosystems with Mascot as a search engine and SwissProt as a database was used to identify proteins based on the recorded peptide mass fingerprinting (PMF) spectra of the protein samples. The search was performed based on the monoisotopic MH^+ mass values of peptides while the missed cleavages of peptides were allowed up to 1.

3. Results and discussion

Because GO sheets have a great amount of negatively charged carboxylic groups on their surface,[11] Co^{2+} tends to be attracted on them by electrostatic interactions. The GO sheets bearing Co(II) ions can be reduced by using suitable reducing agents to form the magnetic graphene–CoMS hybrid. In this work, potassium borohydride or sodium borohydride was employed to initiate the chemical reduction of GO sheets and cobalt ions in a hydrazine-containing aqueous solution. After the mixture was heated at 80 °C for 60 min, the magnetic black hybrid was separated for the following characterization and enrichment of peptides and proteins. When 4 mg of the prepared hybrid was dispersed in 4 mL of water, it could remain in the suspension for at least 1 h without visible sediment (the left inset in Fig. 1A). The dispersed hybrid could be separated to the wall within 1 min with the aid of an NdFeB magnet (~3000 Gs) (the right inset in Fig. 1A). The redispersion and separation processes could be repeated readily. The high dispersibility and sensitivity to a magnetic field exhibited by the hybrid indicates great promise for the convenient enrichment of proteins and peptides.

A vibrating sample magnetometer was used to record the hysteresis loops of the prepared graphene–CoMS hybrid at room temperature to characterize its magnetic properties (Fig. 1A). The saturation magnetizations (M_s), coercivities (H_c) and remanent magnetizations (M_r) of the hybrid are determined to be 80.74 emu g^{-1}, 377.1 Oe, and 10.31 emu g^{-1}, respectively. The presence of H_c and M_r in the hysteresis loops indicates that the hybrid exhibits ferromagnetic behavior. The

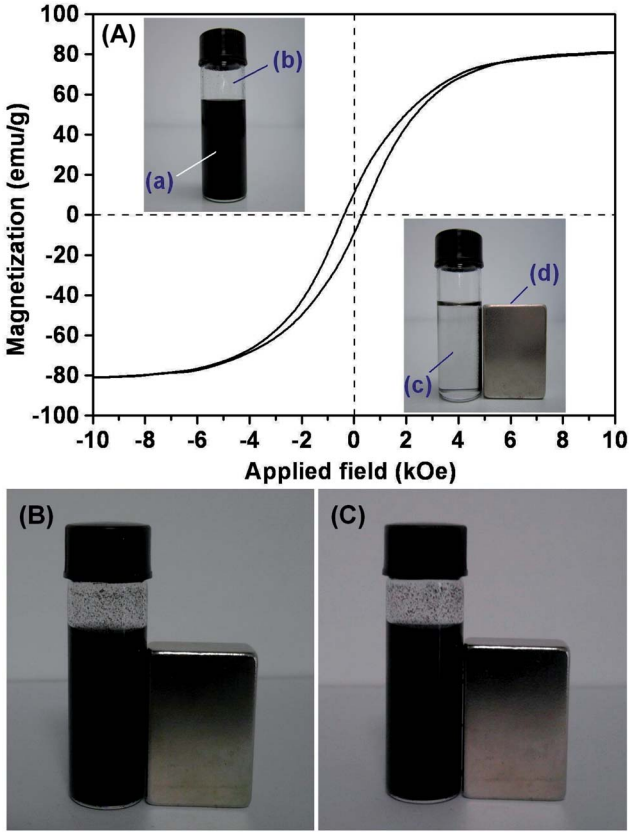

Fig. 1 (A) Hysteresis loops of the graphene–CoMS hybrid and (B and C) the magnetic response of the 1 mg mL^{-1} hybrid prepared by reducing the mixture of GO sheets and cobalt(II) chloride in a hydrazine-containing aqueous solution at 90 °C for 60 (B) and 240 (C) min in the absence of potassium borohydride. Also shown in the insets of Fig. 1A are photographs illustrating the dispersion (left inset) and magnetic separation (right inset) processes of a suspension of the 1 mg mL^{-1} graphene–CoMS hybrid in water. (a) Graphene–CoMS hybrid suspension in water; (b) glass vial; (c) water; (d) NdFeB magnet (~3000 Gs).

ferromagnetism of the graphene–CoMS hybrid can be attributed to its CoMS component. The saturation magnetization of the CoMSs in the hybrid is calculated to be 121.11 emu g^{-1} based on the content of cobalt in the hybrid (2/3, w/w). It is lower than the reported value of bulk cobalt (168 emu g^{-1})[40] owing to the small particle size and the inevitable surface oxidation of CoMSs in the hybrid.[41]

For comparison, hydrazine was also employed to reduce the mixture of GO sheets and cobalt(II) chloride in a hydrazine-containing aqueous solution at 90 °C in the absence of potassium borohydride. Other conditions were the same as those for borohydride-initiated reduction. As illustrated in Fig. 1B and C, the prepared hybrids exhibited no obvious response when the NdFeB magnet was placed close beside the vial for 30 min. Obviously, borohydride could imitate the formation of the magnetic graphene–CoMS hybrid at a lower temperature of 80 °C.

The morphology of the prepared graphene–CoMS hybrid was examined by SEM and TEM. As a characteristic profile of graphene sheets, a crumpled silk wave-like morphology is observed in the SEM and TEM images of the hybrid (Fig. 2d, e and S1a†). Monodispersed CoMSs are individually decorated on the surface of graphene nanosheets. As illustrated in Fig. 2f, the average size of the CoMSs on graphene sheets is estimated to be ~590 nm. CoMSs are well dispersed and embedded throughout the graphene matrix. The SEM image of pristine CoMSs indicates that the size of most CoMSs is in the range of 200 to 400 nm with the average size of ~320 nm (Fig. 2a–c). In comparison with pristine CoMSs, the aggregation of CoMSs in the graphene–CoMS hybrid is significantly reduced owing to their interactions with graphene sheets and the steric hindrance of graphene sheets. Although the hybrid had been sonicated in ethanol before TEM measurements, some CoMSs are found on the surface of graphene sheets, indicating the strong interaction between CoMSs and graphene nanosheets. During the preparation of the graphene–CoMS hybrid, GO sheets played roles of a dispersant, a two-dimensional growth template for CoMSs, and a precursor of graphene.

The EDS spectrum of the prepared graphene–CoMS hybrid was recorded to investigate the element constituents (Fig. S1b†). Because a layer of gold was sputtered on it to record the SEM image, the peaks of gold were also found. The results indicate that the graphene–CoMS hybrid is mainly composed of cobalt, carbon and oxygen elements. Based on the fact that no peak of cobalt hydroxide is observed in the XRD patterns of the hybrid (Fig. S2b†), the oxygen element in the material mainly comes from the residual oxygen-containing functional groups (such as epoxy and hydroxyl groups) on the graphene sheets as well as the oxygen and water molecule absorbed in the hybrid.

The FT-IR spectra of graphene, graphene–CoMS hybrid, graphene–CoMS hybrid, CoMSs, and GO are illustrated in Fig. S3.† As illustrated in Fig. S3d,† absorption bands of GO are observed at 3412, 1730, and 1053 cm^{-1}, which are attributed to the stretching vibrations of O–H, C=O, and C–O–C, respectively. The peaks at 1624, 1407 and 1224 cm^{-1} correspond to the vibration of carboxyl groups.[15] Fig. S3a and S3b† indicate that these peaks become weak or disappear when GO is reduced to graphene by hydrazine. The FT-IR spectrum of the graphene–CoMS hybrid is similar to that of graphene although the peaks of CoMSs below 750 cm^{-1} can be observed, implying that the amount of hydroxyl, carbonyl and carboxyl groups in graphene and the graphene–CoMS hybrid substantially decreases after chemical reduction.

Thermogravimetry was employed to evaluate the weight fraction of graphene in the prepared hybrid. Fig. S3e and S3f† show the TGA curves of graphene and the graphene–CoMS hybrid in air. The weight of the hybrid starts to increase at 300 °C owing to the oxidation of CoMSs in the hybrid. In comparison with the TGA curves of pristine graphene, the obvious weight loss of the hybrid in the temperature range of 470 to 580 °C can be attributed to the decomposition and combustion of graphene. When the hybrid is heated to above 580 °C in air, its graphene component burns completely while the metallic cobalt in it is oxidized to form Co_3O_4.[42] Based on the TGA curve of the hybrid and the molecular weight of Co_3O_4,

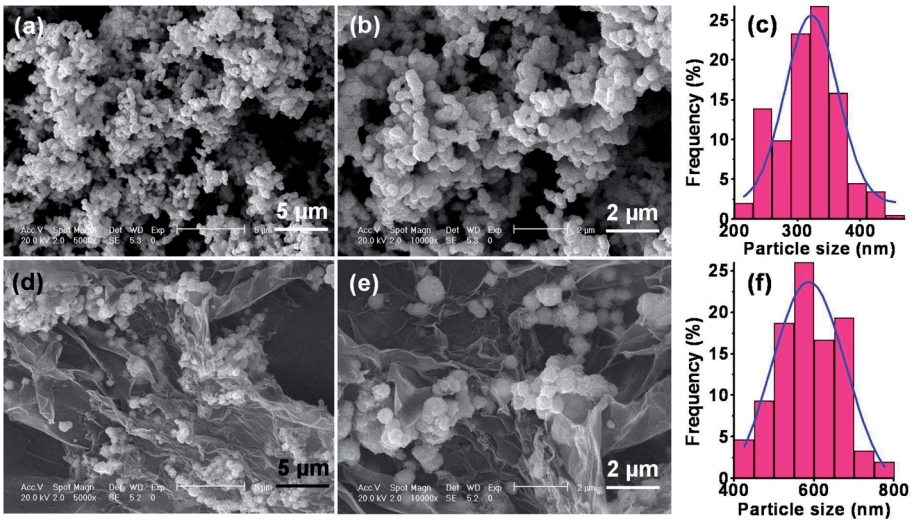

Fig. 2 SEM images of (a and b) CoMSs and (d and e) graphene–CoMS hybrid and particle size distribution of (c) pristine CoMSs and (f) CoMSs on graphene sheets (the number of particles counted, 200). Magnification; (a and d) ×5000 and (b and e) ×10 000.

the mass ratio of metallic cobalt to graphene within the hybrid can be estimated to be approximately 2 : 1.

Fig. S2† illustrates the XRD patterns of graphene and the graphene–CoMS hybrid. Diffraction peaks assigned to graphene at 24.2° (corresponding to the indices of (002))[43] can be clearly seen for both graphene and the graphene–CoMS hybrid, indicating that the graphene structure was not destroyed after chemical reduction. In the XRD pattern of the graphene–CoMS hybrid, all the four characteristic diffraction peaks at 41.9°, 44.7°, 47.7° and 75.1° can be attributed to the (111), (200) and (220) crystalline planes of the hexagonal cobalt (JCPDS 05-0727). The results are good in agreement with the data in a previous report.[44] It can be concluded that the hybrid prepared by the *in situ* chemical reduction of GO sheets and Co(II) ions is a hybrid of graphene and cobalt and no characteristic peaks of $Co(OH)_2$ is observed. It has been reported that cobalt nanoparticles are readily oxidized to paramagnetic Co_2O_3 nanoparticles (average size, ~20 nm).[45] However, both the results TGA and XRD for the hybrid indicate that the cobalt element in it mainly exists in the form of zero-valent cobalt, which implies that the oxidation of CoMSs in the hybrid is not pronounced. The size of the CoMSs in the hybrid is in the range of 400 to 800 nm, which is much higher than that of the reported cobalt nanoparticles (less than 20 nm). The specific surface area of the CoMSs prepared in this work is lower so that the oxidation degree is significantly reduced. More importantly, graphene sheets may protect the CoMSs in the hybrid from oxidation because CoMSs are embedded throughout graphene matrix (Fig. 2d and e).

In this work, Raman spectroscopy was employed to characterize the ordered and disordered crystal structures of graphene in the hybrid. Two Raman peaks at around 1560 and 1360 cm^{-1}, which correspond to G and D bands, were observed in the Raman spectra of GO and the graphene–CoMS hybrid (Fig. S4†). The G band can be attributed to the bond stretching of all pairs of sp^2 bonded carbon atoms while the D band is related to the disordered carbon atoms.[46] The intensity ratio of the D to the G band (I_D/I_G) is related to the average size of sp^2 carbon domains.[47] After chemical reduction of GO sheets, the size of the reestablished conjugated sp^2 carbon domains is usually smaller than that of the original graphite layer, which results in the increase of the I_D/I_G ratio.[48] Such a change is also observed in Fig. S4,† in which the I_D/I_G ratio of the graphene in the hybrid (1.62) is higher than that of GO (1.29). It has been demonstrated that the increase in the ratio of D to G band intensity (I_D/I_G) can be attributed to an increase in the number of isolated sp^2 domains.[47,49] Meanwhile, the D and G bands in the Raman spectrum of the hybrid shift toward lower frequency slightly, which indicates that GO is reduced to form graphene in the hybrid as the layer thickness increases.[50]

In addition, the nitrogen adsorption–desorption isotherms (Fig. 3) and pore size distribution (Fig. S5†) of graphene, graphene–CoMS hybrid and CoMSs were measured to investigate their surface properties. Obviously, the isotherms of the three materials can be assorted as type IV according to the IUPAC classification. The existence of distinct hysteresis loops indicates that they possess nanoporous structures.[51] Table 1

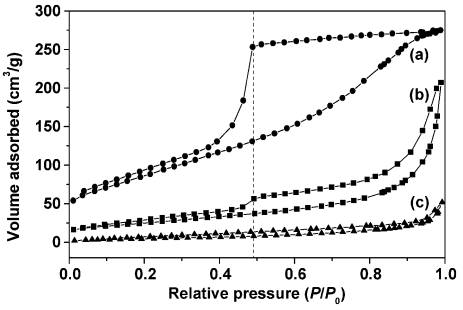

Fig. 3 Nitrogen adsorption–desorption isotherms of (a) graphene, (b) GR–CoMS hybrid, and (c) CoMSs at 77 K.

Table 1 Porous structure parameters of graphene, graphene–CoMs hybrid, and CoMSs

Sample	BET surface area ($m^2\ g^{-1}$)	BJH cumulative pore volume ($cm^3\ g^{-1}$)	BJH pore diameter (nm)
Graphene	316.94	0.4738	3.83
Graphene–CoMS hybrid	89.53	0.3314	3.84
CoMSs	17.88	0.0911	2.36

summarizes the BET surface area, BJH cumulative pore volume and BJH pore diameter of graphene, graphene–CoMS hybrid and CoMSs. The BET surface area of the graphene–CoMS hybrid (89.53 $m^2\ g^{-1}$) is much higher than that of CoMSs (17.88), which is important for the enrichment of proteins and peptides. However, it is lower than that of graphene (316.94 $m^2\ g^{-1}$). The BJH pore size distribution of the three samples is calculated and shown in Fig. S5.† The pore size of graphene is mainly in the range of 2.0 to 4.5 nm. However, the pore size range of the graphene–CoMS hybrid is broadened to the range of 1.4 to 70.0 nm owing to the presence of CoMSs. Although the most probable pore size of the graphene–CoMS hybrid (3.84 nm) is similar to that of graphene (3.83 nm), it is higher than that of CoMSs (2.36 nm). The BJH cumulative pore volume of the graphene–CoMS hybrid (0.3314 $cm^3\ g^{-1}$) is almost 70% of the value for pristine graphene (0.4738 $cm^3\ g^{-1}$) although the mass fraction of graphene in the hybrid is ~33%. The results indicate that CoMSs in the hybrid may enlarge the interplanar spacing between graphene sheets.

The graphene–CoMS hybrid consists of magnetic CoMSs and hydrophobic graphene sheets that have high specific surface area, indicating great promise for the rapid enrichment of peptides and proteins. In this work, it was dispersed in a mixture solution containing Cyt-c and LYZ (1 ng μL^{-1} each) to investigate its enrichment performance. As indicated in Fig. 4a, the signals of the two proteins in the MALDI-TOF mass spectrum are very low prior to enrichment. The signal-to-noise (S/N) ratios are measured to be 15.14 and 8.95 for Cyt-c and LYZ (Fig. 4a). After the mixture is enriched by the magnetic hybrid, the S/N ratios of Cyt-c and LYZ in the eluent significantly increase to 5192.31 and 2894.83 (Fig. 4b). Obviously, the signals of both proteins are dramatically enhanced after enrichment. Both proteins can be easily identified based on the determined molecular mass (12 362 Da for Cyt-c ($[M + H]^+$) and 14 307 Da for LYZ ($[M + H]^+$)). The results indicate that the graphene–CoMS hybrid exhibits satisfactory performance in enriching low-abundance proteins.

To evaluate the enrichment capability of the graphene–CoMS hybrid to peptides, it was employed to capture peptides in the tryptic digests of HEM and Cyt-c (0.5 ng μL^{-1}) for MS-based peptide mapping and protein identification. As indicated in Fig. 5a and c, only 1 or 2 peptides are detected in the digests before enrichment and the proteins cannot be identified. Fig. 5b and d show the mass spectra for the tryptic digests of HEM and Cyt-c after being enriched with the graphene–CoMS hybrid. Clear peptide mass fingerprintings were obtained with significantly enhanced signals. All the identified peptides in both digests are summarized in Tables 2 and 3. The numbers of

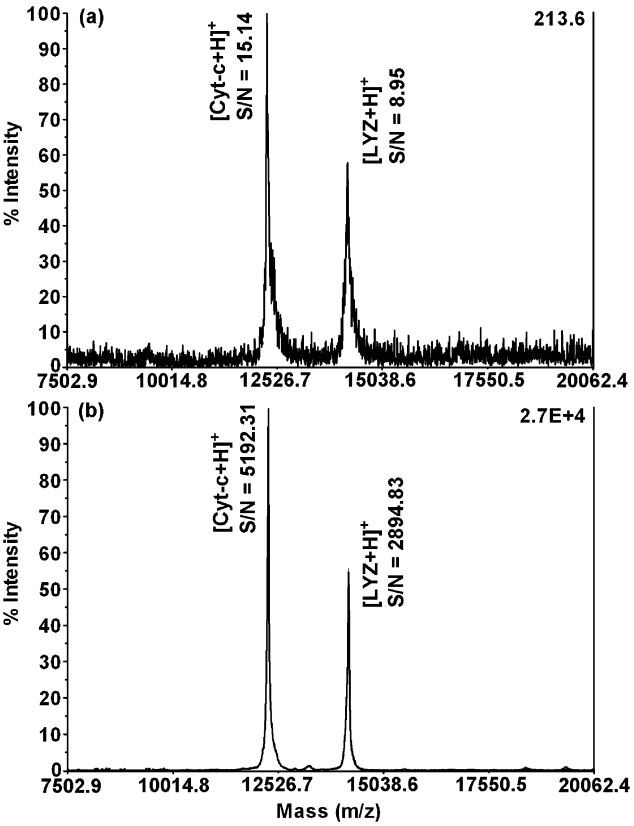

Fig. 4 MALDI-TOF mass spectra of a mixture containing Cyt-c and LYZ (1 ng μL^{-1} each) (a) before and (b) after enrichment with the graphene–CoMS hybrid.

the matched peptides and the amino-acid sequence coverages are 14 and 90% for HEM and 12 and 91% for Cyt-c. In addition, 131 out of the 145 possible amino acids of HEM and 95 out of the 105 possible amino acids of Cyt-c have been identified. The results indicated that both protein samples are positively identified after being enriched by the graphene–CoMS hybrid, implying that it is an ideal magnetic material for the convenient and efficient enrichment of low-abundance proteins and peptides.

In addition, pristine CoMSs were employed to enrich the peptides of HEM and Cyt-c as a control experiment. Fig. S6† illustrates the MALDI-TOF mass spectra of the tryptic digests of HEM and Cyt-c (0.5 ng μL^{-1} each) after being enriched with pristine CoMSs. Only one peptide was found matched in the PMF of HEM while no peak of tryptic peptides was observed in the mass spectra for the digest of Cyt-c. Obviously, the high

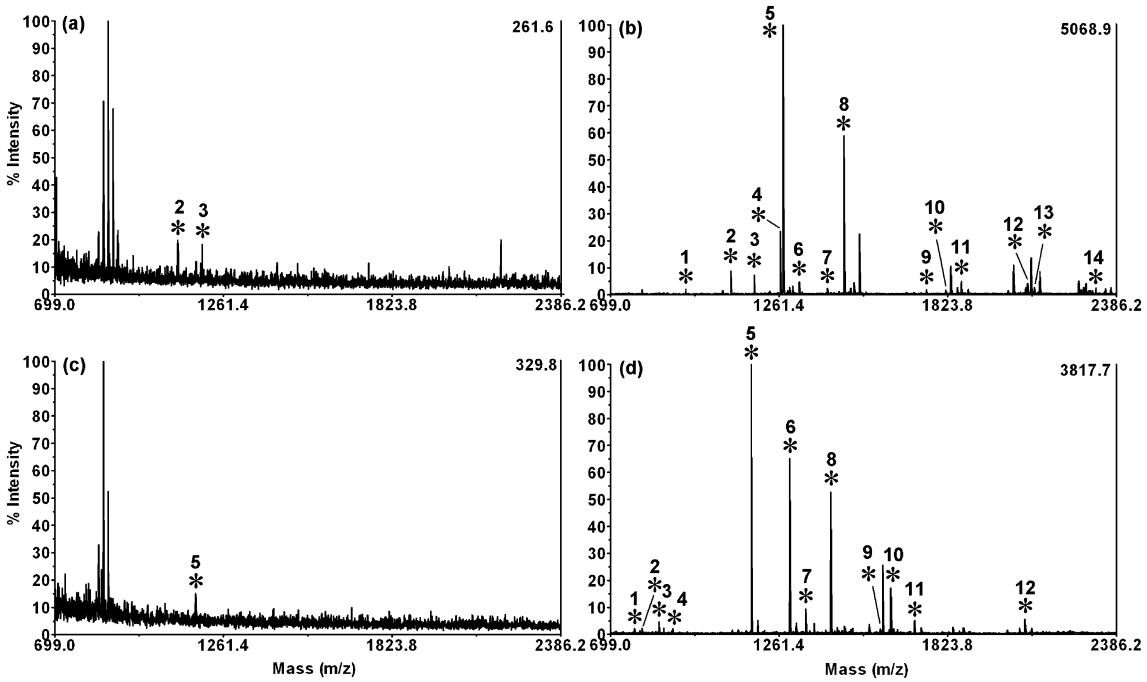

Fig. 5 MALDI-TOF mass spectra of the tryptic digests of (a and b) HEM and (c and d) Cyt-c (0.5 ng μL^{-1} each) before (a and c) and after (b and d) enrichment with the graphene–CoMS hybrid. The peaks marked with asterisks represent the identified peptides in the tryptic digests of proteins.

Table 2 Peptide mapping results for the tryptic digests of 0.5 ng μL^{-1} HEM before and after enrichment[a]

No.	Position	Peptide	Before enrichment	After enrichment
1	8–16	AAVTAFWGK		•
2	19–29	VDEVGGEALGR	•	•
3	8–18	AAVTAFWGKVK	•	•
4	104–115	LLGNVLVVVLAR		•
5	30–39	LLVVYPWTQR		•
6	17–29	VKVDEVGGEALGR		•
7	120–131	EFTPVLQADFQK		•
8	132–145	VVAGVANALAHRYH		•
9	1–16	MLTAEEKAAVTAFWGK		•
10	66–81	VLDSFSNGMKHLDDLK		•
11	116–131	NFGKEFTPVLQADFQK		•
12	40–58	FFESFGDLSTADAVMNNPK		•
13	76–94	HLDDLKGTFAALSELHCDK		•
14	40–60	FFESFGDLSTADAVMNNPKVK		•
Sequence coverage (%)			15	90
Peptides matched			22	14
Amino acids identified			2	131

[a] The matched peptides are labeled with "•".

enrichment capability of the graphene–CoMS hybrid can be attributed to its graphene component that has large surface area, hydrophobic surface, high dispensability, and the unique structure. Peptides and proteins in sample solutions can be enriched on the surface of the hybrid *via* hydrophobic interactions, π–π interactions, and van der Waals force.[37,38] The excellent ferromagnetic properties of the hybrid originate from its cobalt component so that it can be easily separated from the solution.

To test the stability of the prepared graphene–CoMS hybrid, it was sealed in a polypropylene tube and stored in a glass desiccator containing blue silica gel beads at room temperature for 8 months. No obvious change in its weight and saturation magnetization was observed, implying that the stability of the hybrid was satisfactory under the storage conditions. More importantly, the hybrid still attained the ability to enrich proteins and peptides 8 months after it was synthesized.

Table 3 Peptide mapping results for the tryptic digests of 0.5 ng μL^{-1} Cyt-c before and after enrichment[a]

No.	Position	Peptide	Before enrichment	After enrichment
1	81–87	MIFAGIK		•
2	74–80	KYIPGTK		•
3	1–8	MGDVEKGK		•
4	81–88	MIFAGIKK		•
5	29–39	TGPNLHGLFGR	•	•
6	29–40	TGPNLHGLFGRK		•
7	90–100	TEREDLIAYLK		•
8	27–39	HKTGPNLHGLFGR		•
9	40–54	KTGQAPGFTYTDANK		•
10	10–23	IFVQKCAQCHTVEK		•
11	41–56	TGQAPGFTYTDANKNK		•
12	57–73	GITWKEETLMEYLENPK		•
Sequence coverage (%)			10	91
Peptides matched			1	12
Amino acids identified			11	95

[a] The matched peptides are labeled with "•".

4. Conclusions

A novel approach has been developed for the rapid preparation of the graphene–CoMS hybrid at a low temperature of 80 °C by the borohydride-initiated reduction of GO sheets and cobalt(II) chloride in a hydrazine-containing aqueous solution. CoMSs have been successfully decorated on graphene nanosheets with the diameter in the range from 500 to 800 nm. As precursors of graphene, GO sheets act as two-dimensional growth templates for CoMSs, resulting in the *in situ* deposition of CoMSs and simultaneous reduction of GO nanosheets. The graphene–CoMS hybrid displays ferromagnetic behavior at room-temperature and should find a wide range of applications. Moreover, the magnetic hybrid has been successfully employed in the enrichment and identification of low-abundance proteins and peptides in combination with MALDI-TOF MS. The advantages of the graphene–CoMS hybrid as an enrichment material include excellent magnetic responsibility, large surface area, high dispersibility, low expense of preparation, ease of operation, and satisfactory reproducibility, indicating great promise for a wide range of applications.

Acknowledgements

This work was financially supported by the State Oceanic Administration of China (201105007), NSFC (21375023 and 21075020) and Shanghai Science Committee (12441902900).

References

1 K. S. Novoselov, A. K. Geim, S. V. Morozov, D. Jiang, Y. Zhang, S. V. Dubonos, I. V. Grigorieva and A. A. Firsov, *Science*, 2004, **306**, 666.
2 L. Y. Feng, L. Wu and X. G. Qu, *Adv. Mater.*, 2013, **25**, 168.
3 C. N. R. Rao, A. K. Sood, K. S. Subrahmanyam and A. Govindaraj, *Angew. Chem., Int. Ed.*, 2009, **48**, 7752.
4 A. K. Geim, *Angew. Chem., Int. Ed.*, 2011, **50**, 6966.
5 X. Wang, J. Y. Li, W. D. Qu and G. Chen, *J. Chromatogr. A*, 2011, **1218**, 5542.
6 M. Pumera, *Chem. Commun.*, 2011, **47**, 5671.
7 Y. Lu, X. Wang, D. F. Chen and G. Chen, *Electrophoresis*, 2011, **32**, 1906.
8 Q. W. Chen, L. Y. Zhang and G. Chen, *Anal. Chem.*, 2012, **84**, 171.
9 W. D. Qu, L. Y. Zhang and G. Chen, *Biosens. Bioelectron.*, 2013, **42**, 430.
10 K. S. Novoselov, V. I. Falko, L. Colombo, P. R. Gellert, M. G. Schwab and K. Kim, *Nature*, 2012, **490**, 192.
11 O. C. Compton and S. T. Nguyen, *Small*, 2010, **6**, 711.
12 F. H. Li, H. F. Yang, C. S. Shan, Q. X. Zhang, D. X. Han, A. Ivaska and L. Niu, *J. Mater. Chem.*, 2009, **19**, 4022.
13 R. Pasricha, S. Gupta and A. K. Srivastava, *Small*, 2009, **5**, 22539.
14 M. Giovanni, H. L. Poh, A. Ambrosi, G. Zhao, Z. Sofer, F. Saněk, B. Khezri, R. D. Webster and M. Pumera, *Nanoscale*, 2012, **4**, 5002.
15 H. T. Hu, X. B. Wang, F. M. Liu, J. C. Wang and C. H. Xu, *Synth. Met.*, 2011, **161**, 404.
16 G. Yu, L. Hu, M. Vosgueritchian, H. Wang, X. Xie, J. R. McDonough, X. Cui, Y. Cui and Z. Bao, *Nano Lett.*, 2011, **11**, 2905.
17 H. B. Yang, G. H. Guai, C. X. Guo, Q. L. Song, S. P. Jiang, Y. L. Wang, W. Zhang and C. M. Li, *J. Phys. Chem. C*, 2011, **115**, 12209.
18 Q. Xie, Y. T. Qian, S. Zhang, S. Fu and W. Yu, *Eur. J. Inorg. Chem.*, 2006, **12**, 2454.
19 L. Guo, F. Liang, X. Wen, S. Yang, L. He, W. Zheng, C. Chen and Q. Zhong, *Adv. Funct. Mater.*, 2007, **17**, 425.
20 S. Stankovich, D. A. Dikin, G. H. B. Dommett, K. M. Kohlhaas, E. J. Zimney, E. A. Stach, R. D. Piner, S. T. Nguyen and R. S. Ruoff, *Nature*, 2006, **442**, 282.
21 Y. J. Yao, C. Xu, J. C. Qin, F. Y. Wei, M. N. Rao and S. B. Wang, *Ind. Eng. Chem. Res.*, 2013, **52**, 17341.

22 Y. J. Chen, Q. S. Wang, C. L. Zhu, P. Gao, Q. Y. Ouyang, T. S. Wang, Y. Ma and C. W. Sun, *J. Mater. Chem.*, 2012, **22**, 5924.
23 L. Wang, D. L. Wang, X. C. Hua, J. S. Zhu and X. S. Liang, *Electrochim. Acta*, 2012, **76**, 282.
24 L. Wang, J. Li, C. Mao, L. Zhang, L. Zhao and Q. Jiang, *Dalton Trans.*, 2013, **42**, 8070.
25 F. He, N. Niu, F. Qu, S. Wei, Y. Chen, S. Gai, P. Gao, Y. Wang and P. Yang, *Nanoscale*, 2013, **21**, 8507.
26 F. Zhang, C. Y. Hou, Q. H. Zhang, H. Z. Wang and Y. G. Li, *Mater. Chem. Phys.*, 2012, **135**, 826.
27 L. Zhang, Y. Huang, Y. Zhang, Y. F. Ma and Y. S. Chen, *J. Nanosci. Nanotechnol.*, 2013, **13**, 1129.
28 H. Kawasaki, K. Nakai, R. Arakawa, E. K. Athanassiou, R. N. Grass and W. J. Stark, *Anal. Chem.*, 2012, **84**, 9268.
29 J. Yan, T. Wei, J. Feng, Z. J. Fan, L. J. Zhang and F. Wei, *Carbon*, 2012, **50**, 2356.
30 S. Q. Yang, P. Gao, D. Bao, Y. J. Chen, L. Q. Wang, P. P. Yang, G. B. Li and Y. Z. Sun, *J. Mater. Chem. A*, 2013, **1**, 6731.
31 Y. P. He, J. B. Zheng and S. Y. Dong, *Analyst*, 2012, **137**, 4841.
32 P. Kahn, *Science*, 1995, **270**, 369.
33 N. L. Anderson and N. G. Anderson, *Electrophoresis*, 1998, **19**, 1853.
34 H. M. Chen, C. H. Deng and X. M. Zhang, *Angew. Chem., Int. Ed.*, 2010, **49**, 607.
35 H. M. Chen, C. H. Deng, Y. Li, Y. Dai, P. Y. Yang and X. M. Zhang, *Adv. Mater.*, 2009, **21**, 2200.
36 L. Zhang, S. Z. Qiao, Y. G. Jin, H. G. Yang, S. Budihartono, F. Stahr, Z. F. Yan, X. L. Wang, Z. P. Hao and G. Q. Lu, *Adv. Funct. Mater.*, 2008, **18**, 3203.
37 Q. Liu, J. B. Shi, J. T. Sun, T. Wang, L. X. Zeng and G. B. Jiang, *Angew. Chem., Int. Ed.*, 2011, **50**, 5913.
38 Q. Liu, B. J. Shi, M. T. Cheng, G. L. Li, D. Cao and G. B. Jiang, *Chem. Commun.*, 2012, **48**, 1874.
39 H. Z. Fan, H. M. Bao, L. Y. Zhang and G. Chen, *Proteomics*, 2011, **11**, 3420.
40 G. X. Zhu, X. W. Wei, C. J. Xia and Y. Ye, *Carbon*, 2007, **45**, 1160.
41 S. Deka, A. Falqui, G. Bertoni, C. Sangregorio, G. Poneti, G. Morello, M. De Giorgi, C. Giannini, R. Cingolani, L. Manna and P. D. Cozzoli, *J. Am. Chem. Soc.*, 2009, **131**, 12817.
42 Z. S. Wu, W. Ren, L. Gao, J. Zhao, Z. Chen, B. Liu, D. Tang, B. Yu, C. Jiang and H. M. Cheng, *ACS Nano*, 2009, **3**, 411.
43 Y. Wang, Y. M. Li, L. H. Tang, J. Lu and J. H. Li, *Electrochem. Commun.*, 2009, **11**, 889.
44 Z. Y. Ji, X. P. Shen, Y. Song and G. X. Zhu, *Mater. Sci. Eng., B*, 2011, **176**, 711.
45 T. L. Wee, B. D. Sherman, D. Gust, A. L. Moore, T. A. Moore, Y. Liu and J. C. Scaiano, *J. Am. Chem. Soc.*, 2011, **133**, 16742.
46 F. Tuinstra and J. L. Koenig, *J. Chem. Phys.*, 1970, **53**, 1126.
47 S. Stankovich, D. A. Dikin, R. D. Piner, K. A. Kohlhaas, A. Kleinhammes, Y. Y. Jia, Y. Wu, S. T. Nguyen and R. S. Ruoff, *Carbon*, 2007, **45**, 1558.
48 C. Xu, X. Wang and J. W. Zhu, *J. Phys. Chem. C*, 2008, **112**, 19841.
49 S. Stankovich, R. D. Piner, X. Q. Chen, N. Q. Wu, S. T. Nguyen and R. S. Ruoff, *J. Mater. Chem.*, 2006, **16**, 155.
50 A. C. Ferrari, *Solid State Commun.*, 2007, **143**, 47.
51 G. Gund, D. P. Dubal, B. H. Patil, S. S. Shinde and C. D. Lokhande, *Electrochim. Acta*, 2013, **92**, 205.